

# Structural investigation of graphitic carbon nitride *via* XRD and Neutron Diffraction

Federica Fina<sup>†</sup>, Samantha K. Callear<sup>‡</sup>, George M. Carins<sup>†</sup>, John T. S. Irvine<sup>†\*</sup>

<sup>†</sup> School of Chemistry, University of St Andrews, St Andrews, KY16 9ST, Scotland, United Kingdom

<sup>‡</sup> ISIS Neutron and Muon Facility, STFC, Rutherford Appleton Laboratory, Harwell Oxford, Didcot OX11 0QX, United Kingdom

**ABSTRACT:** Graphitic carbon nitride ( $g\text{-C}_3\text{N}_4$ ) has, since 2009, attracted great attention for its activity as a visible light-active photocatalyst for hydrogen evolution. Since it was synthesized in 1834,  $g\text{-C}_3\text{N}_4$  has been extensively studied both catalytically and structurally. While its 2D structure seems to have been solved, its 3D crystal structure has not yet been confirmed. This study attempts to solve the 3D structure of graphitic carbon nitride by means of x-ray diffraction and of neutron scattering. Initially, various structural models are considered and their XRD patterns compared to the measured one. After selecting possible candidates as  $g\text{-C}_3\text{N}_4$  structure, neutron scattering is employed to identify the best model that describes the 3D structure of graphitic carbon nitride. Parallel chains of tri-*s*-triazine units organized in layers with an A-B stacking motif are found to describe the structure of the synthesized graphitic carbon nitride well. A misalignment of the layers is favorable because of the decreased  $\pi$ - $\pi$  repulsive *inter*-layer interactions.

## INTRODUCTION

Graphitic carbon nitride ( $g\text{-C}_3\text{N}_4$ ) is one of the several allotropes of the carbon nitrides family. It was synthesised for the first time by Berzelius and named “melon” by Liebling in 1834.<sup>1</sup> It is a polyconjugated semiconductor composed of carbon and nitrogen atoms and it is characterised by a layered graphitic-like structure.<sup>2</sup> The fully polymerised form of  $g\text{-C}_3\text{N}_4$ , characterised by a C:N ratio of 0.75, cannot be practically obtained. Therefore, the material presents a hydrogen content of 1-2 %, which varies depending on the synthesis procedure.<sup>3</sup> Graphitic carbon nitride can be easily synthesised via solid state synthesis from cheap materials such as melamine, it is insoluble in most solvents and shows great stability in extreme conditions (pH = 0 and pH = 14).<sup>2, 4</sup> Due to these characteristics, it has recently attracted great attention for different catalytic applications, in particular photocatalysis for hydrogen evolution from water.<sup>2, 4</sup> Even though widely studied as a catalyst, to date, the  $g\text{-C}_3\text{N}_4$  crystal structure has not been fully solved. The first examples of structural investigation date back to the early 20<sup>th</sup> century.<sup>5-7</sup> Since then two main 2D structures have been suggested: a triazine-based (Figure 1a)<sup>8-11</sup> and a tri-*s*-triazine-based one (Figure 1b)<sup>12-15</sup>. Many investigations have been carried out in order to confirm which of the two structures could describe  $g\text{-C}_3\text{N}_4$ .<sup>12-13, 16-20</sup> By 2009<sup>16, 19</sup>, with the aid of electron diffraction,<sup>16, 19-20</sup> and solid state Nuclear Magnetic Resonance,<sup>16</sup> the 2D structure of  $g\text{-C}_3\text{N}_4$  synthesised by thermal condensation of small organic polymers was considered solved. The structure of  $g\text{-C}_3\text{N}_4$  was confirmed as a tri-*s*-triazine based polymeric structure.<sup>16, 19</sup> However,

due to the highly disordered character of the material an accurate description of its 3D structure had only been suggested.<sup>20-21</sup>

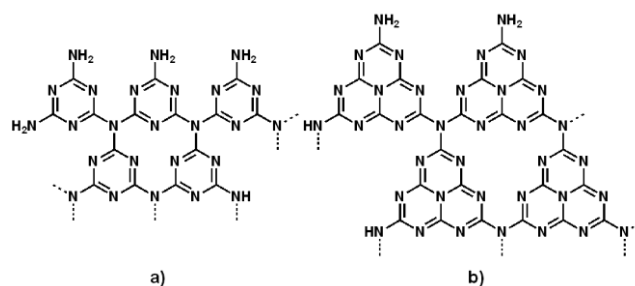


Figure 1 Structures considered representative of  $g\text{-C}_3\text{N}_4$ : a) triazine based and b) tri-*s*-triazine based.

To the best of our knowledge the most recent work on the 3D structure of  $g\text{-C}_3\text{N}_4$  is that of Tyborsky *et al.*<sup>21</sup> In their work x-ray diffraction modelling is employed to solve the structure of graphitic carbon nitride. However, due to the short range order of the material which prevents proper structure refinement, x-ray diffraction alone is not sufficient. Neutron scattering on the other hand can provide additional information useful for the structure determination of  $g\text{-C}_3\text{N}_4$ .

Neutrons interact with the nuclei of the atoms instead of the electrons and can therefore offer complementary information to XRD analysis regarding the atomic structure of materials.<sup>22</sup> Additionally due to the size of the neutrons, neutron scattering is very sensitive to hydrogen and other light elements such as carbon. Due to the op-

posite sign of the scattering lengths of H and D,<sup>23</sup> negative peaks are produced in the first case and positive in the second. A comparison of labelled and not-labelled materials allows for direct identification of atomic correlations involving hydrogen. Neutron scattering can therefore be a suitable analytical technique for g-C<sub>3</sub>N<sub>4</sub> and can offer complementary information to the XRD analysis. In the present work, we employ structural models proposed in the literature, we create some new ones and generate their theoretical XRD patterns. These are then compared to the measured XRD pattern of the synthesised graphitic carbon nitride. After narrowing down the possible crystal structures, the most promising ones are compared with the results from the neutron scattering analysis. It is found that the material synthesised for this study is best described by tri-*s*-triazine layers with an off-set in their alignment. To the best of our knowledge no report of Neutron Scattering on g-C<sub>3</sub>N<sub>4</sub> exists in the literature and this work brings the structural characterisation of this active catalyst a step forward.

## EXPERIMENTAL

**Material synthesis.** Graphitic carbon nitride was synthesised by thermal polycondensation of Melamine (Sigma-Aldrich, 99.9 %) at 500 °C for 15 h. The precursor was placed in a closed alumina crucible and heated to temperature with a rate of 5 °C/min. After the synthesis it was ground to fine powder. To synthesize the deuterated g-C<sub>3</sub>N<sub>4</sub> the same synthetic procedures was applied but Melamine-d<sub>6</sub> was employed as the starting material.

**Photocatalytic performance evaluation.** Measurement of the photocatalytic hydrogen evolution were performed in a custom-made photocatalytic reactor with top irradiation through a quartz window. In a typical experiment 0.1 g of catalyst (1 g·L<sup>-1</sup>) were suspended in 100 mL of a 10 v.% solution of triethanolamine (TEOA)<sup>2</sup> employed as sacrificial agent. The inner atmosphere was purged with Argon gas to remove any trace of air. Top irradiation was carried out with a 250 W iron-doped metal halide ultraviolet-visible lamp ( $\geq 290$  nm; UV Light Technology Limited) with a cut-off filter ( $\geq 420$  nm; Borosilicate Coated Glass, UQG Optics Ltd) to block UV-irradiations. Hydrogen evolution was monitored for an experimental duration of 20 hours using a gas chromatograph (Agilent 3000 Micro Gas Chromatograph).

**X-ray diffraction.** The microstructure was investigated by powder X-Ray Diffraction (XRD) using an Empyrean PANalytical series 2 diffractometer with a Cu K $\alpha$  radiation source ( $\lambda = 1.5406$  Å). The theoretical patterns of the modelled structures were generated using the software FullProf. In order to remove all symmetry operators during the generation of the theoretical patterns, the space group P1 is employed as a mere processing tool.

**Neutron Scattering.** The neutron scattering measurements were performed using NIMROD (InterMediate Range Order Diffractometer) at the ISIS Neutron and Muon Facility, Rutherford Appleton Laboratory, UK. Gra-

phitic carbon nitride was packed into a flat plate TiZr container that was chosen because of the opposite sign of the scattering length of the two elements, giving an overall null scattering.<sup>24</sup> The container had a wall thickness of 1 mm and an inner aperture of 1 mm. The beam size was 3 cm x 3 cm. A Vanadium plate was used as a standard to normalize the data. Measurements of the background and container were also collected and used to correct the raw data. The data normalisation and corrections were carried out using GudrunN.<sup>24</sup> PDFGui was employed to generate calculated PDFs of the crystal structures using scale and damp-ing factors that were fitted to the experimental data. The atomic positions, lattice parameters and isotropic displacement parameters were inputted as per the crystal structure data and were kept fixed.<sup>25</sup> PDFGui outputs a residual curve (the difference between the model and the data) and also the weighted R-factor (Rw) which is a measure of how accurately the model represents the data (the smaller the value the better the fit).

### Elemental Analysis and density measurement.

The elemental analysis was acquired with Carlo Erba Flash 2000 Elemental Analyser, configured for wt.% CHN. Density measurements were carried out with a Micromeritics, AccuPyc 1340 Gas Pycnometer.

## RESULTS

**Photocatalytic performance.** Graphitic carbon nitride is tested for photocatalytic hydrogen evolution under visible light. Triethanolamine (TEOA) is employed as sacrificial agent to promote the production of hydrogen. The material without the aid of a co-catalyst shows an evolution rate at the steady state of less than 1  $\mu\text{mol}\cdot\text{h}^{-1}$  under the described conditions. However, after loading of 1 wt.% of platinum as the co-catalyst the performance reaches a rate of 22  $\mu\text{mol}\cdot\text{h}^{-1}$ . This results are consistent with what has been reported in the literature for graphitic carbon nitride,<sup>2</sup> showing that the material subject of this study is an active photocatalyst for hydrogen evolution.

**XRD analysis.** The x-ray diffraction pattern of g-C<sub>3</sub>N<sub>4</sub> synthesized by thermal polycondensation of melamine is illustrated in Figure 2. The characteristic peaks associated with g-C<sub>3</sub>N<sub>4</sub> can be identified.<sup>2, 14</sup> The main one at  $2\theta = 27.4^\circ$  is reported as the (002) plane, equivalent to a *d*-spacing of 0.326 nm. This is usually ascribed to the distance between the layers of the graphitic material.<sup>2, 14</sup> The peak at  $2\theta = 13.00^\circ$  is attributed to the (100) plane, with a *d*-spacing of 0.680 nm. This is due to the *intra*-layer *d*-spacing.<sup>2, 14</sup>

The measured XRD pattern is initially compared to the crystal structure proposed by Teter and Hemley<sup>8</sup> in 1996 (Figure 2). Even though a fully polymerised g-C<sub>3</sub>N<sub>4</sub> (C:N ratio of 0.75) cannot be obtained, we still asses it for clarity. The proposed structure describes layers of triazine units with a 3D A-B stacking organization and it is characterized by a hexagonal unit cell ( $a = b = 4.7420$  Å,  $c = 6.7205$  Å,  $\alpha = \beta = 90^\circ$ ,  $\gamma = 120^\circ$ ) with space group P $\bar{6}m2$ . Compared to the measured pattern, the (002) re-

flexion is shifted towards lower angles meaning a larger  $d$ -spacing in between the layers; in addition the (100) reflection is significantly shifted compared to that of our  $g$ - $C_3N_4$ , corresponding to an *intra*-layer  $d$ -spacing of 0.41 nm. A similar result was obtained by Tyborski *et al.*<sup>21</sup> for their polymeric carbon nitride (PCN) synthesized from dicyandiamide by double calcination step.<sup>21</sup> The PCN described in their paper is characterized by a more pronounced (100) reflection compared to the material subject of this investigation.

To take into account a fully polymerized tri-*s*-triazine-based  $g$ - $C_3N_4$ , a structure is generated starting from the unit cell proposed by Teter and Hemeley. The new unit cell parameters are:  $a = b = 7.113 \text{ \AA}$ ,  $c = 6.490 \text{ \AA}$ ,  $\alpha = \beta = 90^\circ$ ,  $\gamma = 120^\circ$ . The parameter  $c$  is chosen to match the *inter*-layer spacing of the measured pattern. The theoretical pattern generated from the tri-*s*-triazine structure is compared to the measured pattern in Figure 2. The same reflections seen for the triazine-based structure are present but with a shift towards lower angles. The (100) reflection, being at  $2\theta = 14.38^\circ$  (0.615 nm), does not yet match the measured one. On the other hand its relative intensity is 0.18, very close to the experimental value,  $I_{100}/I_{002} = 0.19$ . The off-set of the (100) reflection and the presence of a strong (101) reflection at  $2\theta = 19.86^\circ$  do not make this a suitable model.

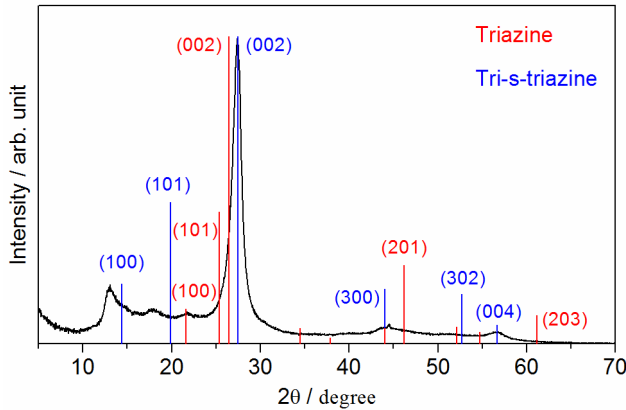


Figure 2 Theoretical patterns for fully polymerized triazine and tri-*s*-triazine based  $g$ - $C_3N_4$ . Triazine unit cell parameters:  $a = b = 4.7420 \text{ \AA}$ ,  $c = 6.7205 \text{ \AA}$ ,  $\alpha = \beta = 90^\circ$ ,  $\gamma = 120^\circ$ ; tri-*s*-triazine unit cell parameters:  $a = b = 7.113 \text{ \AA}$ ,  $c = 6.490 \text{ \AA}$ ,  $\alpha = \beta = 90^\circ$ ,  $\gamma = 120^\circ$

Elemental analysis of the synthesized material reveals a hydrogen content of 1.5 wt.% and a C:N ratio of 0.68. These values confirm a partially polymerized structure. Models of partially polymerized  $g$ - $C_3N_4$  can be obtained by removing tri-*s*-triazine units from the network. With this approach, depending on which units are removed, many different structural models can be generated. Figure 3 compares two different structures: one proposed by Döblinger *et al.*,<sup>19</sup> and one created for this study (atomic coordinates in Table S1). The structure proposed by Döblinger *et al.*,<sup>19</sup> after an electron diffraction study, is characterized by a hexagonal unit cell with cell parameters as

follow:  $a = b = 12.77 \text{ \AA}$ ,  $c = 6.49 \text{ \AA}$ ,  $\alpha = \beta = 90^\circ$  and  $\gamma = 120^\circ$ . The partially polymerized structure created for this study is also characterized by hexagonal unit cell ( $a = b = 13.9246 \text{ \AA}$ ,  $c = 6.49 \text{ \AA}$ ,  $\alpha = \beta = 90^\circ$  and  $\gamma = 120^\circ$ ) and it is obtained from the tri-*s*-triazine structure previously discussed. Both 3D structures are considered with an A-B stacking configuration. Figure 3 shows the theoretical patterns. In both cases, the peaks at low angles are more intense than the (002) reflection. This indicates that these structures as well cannot be considered representative of the synthesized graphitic carbon nitride.

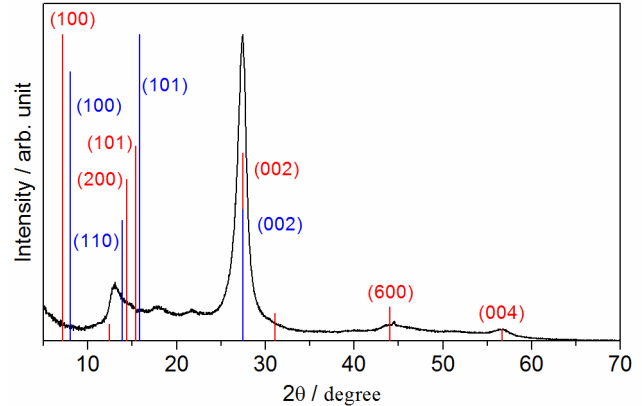


Figure 3 Theoretical XRD patterns for two different partially polymerized graphitic carbon nitride: Döblinger *et al.*<sup>19</sup> (blue,  $a = b = 12.77 \text{ \AA}$ ,  $c = 6.49 \text{ \AA}$ ,  $\alpha = \beta = 90^\circ$  and  $\gamma = 120^\circ$ ) and this study (red,  $a = b = 13.9246 \text{ \AA}$ ,  $c = 6.49 \text{ \AA}$ ,  $\alpha = \beta = 90^\circ$  and  $\gamma = 120^\circ$ ).

An alternative tri-*s*-triazine structure has been proposed by Lostch *et al.*<sup>16, 20</sup> after carrying out an electron diffraction study. The structure is composed of parallel chains of tri-*s*-triazine units (Figure 4 inset) and the authors refer to it as “Melon”.<sup>16</sup> This nomenclature will be employed in the present study to distinguish this and similar structures from other tri-*s*-triazine models; while the synthesised material will still be referred to as  $g$ - $C_3N_4$ . The unit cell of Melon is characterised by an orthorhombic geometry and an A-A staking of the layers. The XRD theoretical pattern of this structure is shown in Figure 4. The unit cell parameter  $c$  was chosen to match the (002) reflection ( $a = 16.7 \text{ \AA}$ ,  $b = 12.4 \text{ \AA}$ ,  $c = 6.49 \text{ \AA}$ ,  $\alpha = \beta = \gamma = 90^\circ$ , Space Group:  $P2_12_12_1$ ). The theoretical pattern generated by this structure is very similar to the measured one. Two major reflections are observed at  $2\theta = 12.78^\circ$  and  $2\theta = 27.46^\circ$ . The reflection at  $2\theta = 12.78^\circ$ , due to the different geometry of the unit cell is now assigned to the (210)<sub>orthorhombic</sub> plane rather than the (100)<sub>hexagonal</sub>. However, this reflection is shifted of  $0.17^\circ$  towards lower angles compared to the measured one, and its intensity relative to the (002) reflection ( $I_{210}/I_{002}$ ) is 0.44, while the experimental value is 0.19. The material employed by Lostch *et al.*<sup>16, 20</sup> was synthesised by thermal polycondensation of melamine, as in the present work, but the reaction is carried out in a sealed ampule. This

will generate a material with a higher level of crystallinity which could justify the small differences in the XRD patterns. This structure is therefore employed as starting point for further improvement. Initially it can be modified to move the peak in the desired position. This can be achieved by “shrinking” the unit cell or by reducing the distance,  $d_c$  (Figure 4 inset), between the polymeric chains. The first approach was applied by Tyborski *et al.*,<sup>21</sup> however, this method causes a contraction of the aromatic network resulting in C=N bond too short.<sup>26-27</sup> The second approach does not affect the aromatic network and therefore is chosen for this investigation. The structure is now described by a unit cell of parameters:  $a = 16.4 \text{ \AA}$ ,  $b = 12.4 \text{ \AA}$ ,  $c = 6.49 \text{ \AA}$ ,  $\alpha = \beta = \gamma = 90^\circ$  (for atomic coordinates see Table S2). The theoretical pattern for the modified Melon is illustrated in Figure 4. All of the experimental reflections find an equivalent in the theoretical pattern. The position of the  $(210)_{\text{orthorhombic}}$  reflection, as expected, matches that of the measured peak. However, its relative intensity is 0.37, still too high.

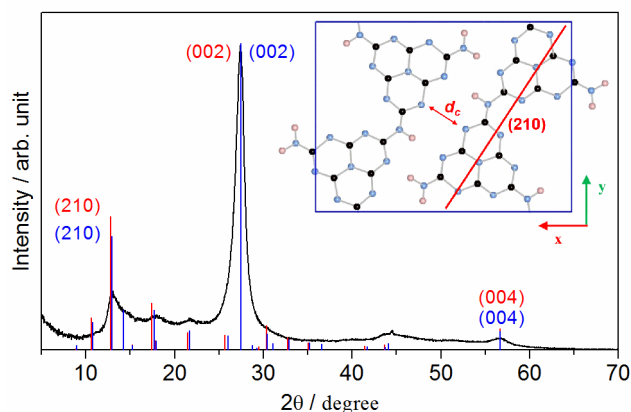


Figure 4 XRD theoretical patterns of Melon as proposed by Lostch *et al.* (red,  $a = 16.7 \text{ \AA}$ ,  $b = 12.4 \text{ \AA}$ ,  $c = 6.49 \text{ \AA}$ ,  $\alpha = \beta = \gamma = 90^\circ$ , Space Group:  $P2_12_12_1$ ) and the modified version of this investigation (blue,  $a = 16.4 \text{ \AA}$ ,  $b = 12.4 \text{ \AA}$ ,  $c = 6.49 \text{ \AA}$ ,  $\alpha = \beta = \gamma = 90^\circ$ ). Inset: structure of Melon.

The modified Melon structure can be further modified to achieve a better match to the real structure. The angles of the orthorhombic unit cell can be increased or decreased to simulate a structural shift of the layers. This would affect the  $(210)_{\text{orthorhombic}}$  reflection which is associated to the alignment of the aromatic layers. Tyborski *et al.*<sup>21</sup> investigated the effect that modifying the angle  $\gamma$  has on the XRD pattern.<sup>21</sup> However, an increase or decrease of this angle would produce a distortion of the aromatic units placed on the  $ab$  planes, rather than a shift of the layers. This is an example of the molecular constraints posed by the structure of graphitic carbon nitride. Here, only  $\alpha$  and  $\beta$  will be modified to investigate the effect of a shift of the layers but maintaining a nominal A-A stacking. The new unit cell will now have a monoclinic geometry. While changing one of the angles, the parameter  $c$  is adjusted to retain the distance between the layers constant at a value of  $2\theta = 27.4^\circ$ . Figure 5 illustrates the effect

that a change in one of the angles has on the position and the relative intensity of the  $(210)_{\text{monoclinic}}$  reflection. The effects produced by varying the intensity of  $\alpha$  or  $\beta$  are found to be very similar. In both cases the intensity slightly decreases from the original 0.37 to  $\sim 0.30$ . The decrease is greater for  $\beta$  (0.30 for  $\beta = 115^\circ$ ) than for  $\alpha$  (0.34 for  $\alpha = 115^\circ$ ) but in both cases this value still remains too high compared to that of  $g\text{-C}_3\text{N}_4$  ( $I_{210}/I_{002} = 0.19$ ). Changing the angle also has an effect on the position of the peak by shifting it towards higher  $2\theta$ . After remaining nearly the same for both  $\alpha$  and  $\beta$  up to  $95^\circ$ , the change is the largest for  $\beta = 115^\circ$  with  $2\theta = 13.90^\circ$ . The effects of the angles below  $90^\circ$  have also been investigated and they were found mirroring the behavior of  $\alpha(\beta) > 90^\circ$ . The optimum value of  $\alpha$  and  $\beta$  can be found between  $82^\circ$  and  $98^\circ$ .

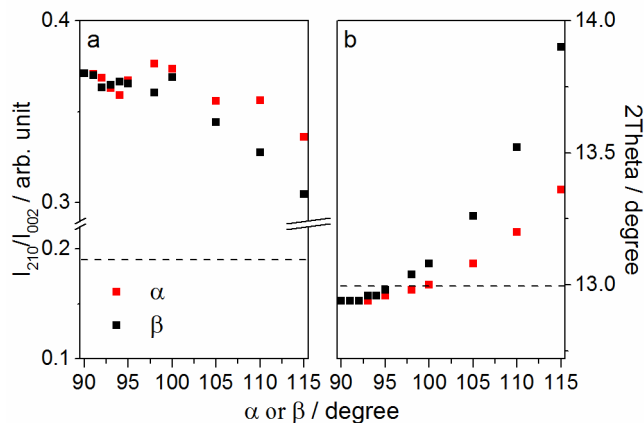


Figure 5 Effect of  $\alpha$  and  $\beta$  on the relative intensity ( $I_{210}/I_{002}$ ) and the position of the  $(210)$  reflection. Dashed lines represents the experimental values.

A different approach is that of actually shifting the layers retaining the orthorhombic geometry and introducing an A-B stacking configuration. Lostch<sup>20</sup> considered three different shifts in her electron diffraction study but concluded that for her material those models did not match the experimental electron diffraction patterns. Here, the different synthesis method applied probably results in a different structure, therefore the proposed shifts are used to generate the XRD theoretical patterns (Figure 6).

The first shift, A, is random along both the  $x$  and  $y$  directions (0.124, -0.244) the second, B, is along the diagonal of the cell (0.072, 0.054) and the third, C, is along the  $y$  axis (0.000, 0.109). The theoretical pattern of modified Melon with shifted layers are compared in Figure 6. While no major differences in the peak position can be observed between the patterns, the relative intensities of some of the reflections, especially the  $(200)$  and  $(210)$ , are found to vary significantly. The reflection  $(200)$  has an  $I_{200}/I_{002}$  intensity of 0.05, 0.07 and 0.09 for Shift A, B and C, respectively. For the  $(210)$  reflection the  $I_{210}/I_{002}$  is 0.16 for Shift A, 0.30 for Shift B and 0.33 for Shift C. While Shift B and Shift C are only marginally decreased, Shift A is in good agreement with the experimental value (0.19), making it the most promising model.

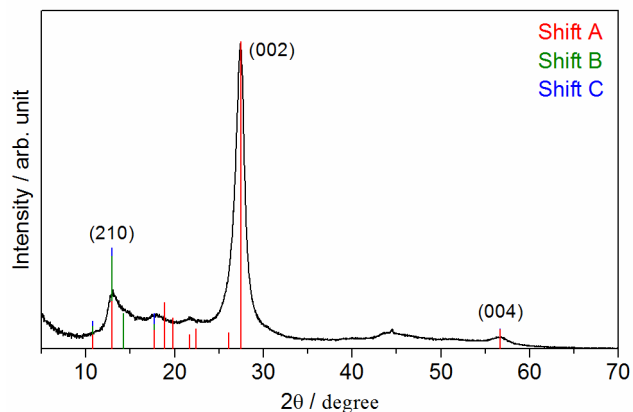


Figure 6 Theoretical XRD patterns of three modified melon structure with shifted layers. Shift A: (0.124, -0.244), Shift B: (0.072, 0.054), Shift C: (0.000, 0.109).

The measured pattern was indexed with the software HighScore Plus to investigate the level of symmetry of the structure. The suggested unit cell is characterised by orthorhombic geometry in agreement with the orthorhombic cell considered for the Melon structure. It was also found that the highest level of symmetry that justifies all the reflections of the experimental pattern is described by the space group Cmmm (Figure S1).

**Neutron scattering analysis.** The structure factor,  $F(Q)$ , measured for the graphitic carbon nitride (Figure S2) is in good agreement with the XRD pattern, showing the (210)<sub>orthorhombic</sub> and the (002)<sub>orthorhombic</sub> reflections. From the Fourier Transform of the structure factor the differential correlation function,  $D(r)$ , is obtained (Figure 7). The  $D(r)$  can be divided into three main sections (I, II and III, Figure 7). Area I includes the distances from 0 Å to 3 Å, these are atomic correlations within the layers of the graphitic carbon nitride materials, more specifically, within a tri-*s*-triazine unit. Examples are the N-H bond at about 1 Å and the C=N bond at 1.33 Å. The second area (II) can be found between 3 Å and 6 Å, where the *inter*-layer distances contribute to the signal, for example the *inter*-layer *d*-spacing at 3.25 Å. In this area long *intra*-planar distances can also be found, for instance the distance between the N<sub>3</sub> and the N<sub>12</sub> (Figure 7-inset) of ~ 4.7 Å. Systematic ripples observed above 6 Å (III) can be attributed to the same moieties found in area II repeated in space. Therefore, from this point on, only areas I and II will be discussed in more details.

Hydrogen and deuterium have scattering lengths of opposite phase<sup>23</sup> that in a  $D(r)$  plot will translate in negative peaks for hydrogen and positive peaks for deuterium. Figure 8 compares the differential correlation functions of hydrogenated and deuterated graphitic carbon nitride. The most evident effect of isotopic labelling is visible at 1 Å which corresponds to the N-H bond distance.<sup>26</sup> This appears in the form of a negative peak for the graphitic carbon nitride and positive for the labelled version (Figure 8). At 2 Å a less pronounced effect of the labelling is

visible. This peak is assigned to the second-neighbor distance H-(N)-C (from H<sub>1</sub> to C<sub>1</sub> in Figure 7). Less obvious differences can be noticed at longer distances: at ~ 3.2 Å in the form of a small shoulder and at ~ 4.6 Å as a change in the peak intensity. The shoulder at ~ 3.2 Å can be associated with the distance between the hydrogen from an amino group to the first nitrogen encountered in the aromatic ring (H<sub>3</sub> to N<sub>5</sub> in Figure 7). The peak at ~ 4.6 Å is more difficult to assign to any specific atomic correlation due to the large amount of possible atomic pairs at this and similar distances.

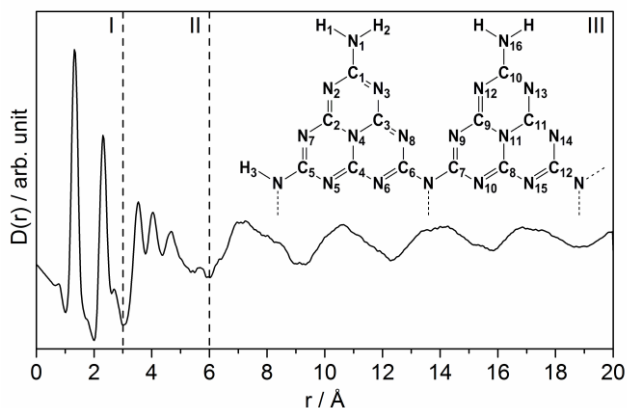


Figure 7  $D(r)$  of graphitic carbon nitride. Inset: tri-*s*-triazine units.

Fitting the data with Gaussian functions for each peak shows that the first positive peak is centred at 1.33 Å. It is due to the partial double bond in the aromatic network, C=N.<sup>26-28</sup> The high symmetry of the peak (Figure 8) suggests the absence of a component at 1.41 Å which would indicate the presence of a  $Csp^2-Nsp^3$  correlation<sup>28</sup> for the C-N bonds bridging the tri-*s*-triazine units. Therefore, the bridging nitrogen atoms feature a  $sp^2$  hybridisation resulting in a shorter bond. At 2.32 Å the second-neighbor correlation for carbon and nitrogen atoms (C<sub>2</sub> to C<sub>4</sub> and N<sub>4</sub> to N<sub>8</sub>, Figure 7 inset) is present. The small peak at 2.70 Å could instead be associated with the correlation between mirroring carbon and nitrogen atoms in the aromatic ring (N<sub>2</sub> to C<sub>3</sub>). The *inter*-layer *d*-spacing in the XRD for the (002) is reported at 3.26 Å. In the differential pair correlation functions  $D(r)$  however isolated peak is seen at 3.26 Å, the first well defined peak in this region appears instead at 3.52 Å which is the correlation between atoms such as N<sub>1</sub> and C<sub>3</sub> (Figure 7 inset). Due to the broad nature of the peaks the correlation at 3.26 Å is not clearly visible which is typical for structures with *inter*-layer disorder, e.g. graphite, as the disordered nature of the layers results in a broad peak. Instead the *inter*layer correlations can be seen as periodic oscillations at high *r* values – these show the *inter*layer spacing to be 3.25 Å.

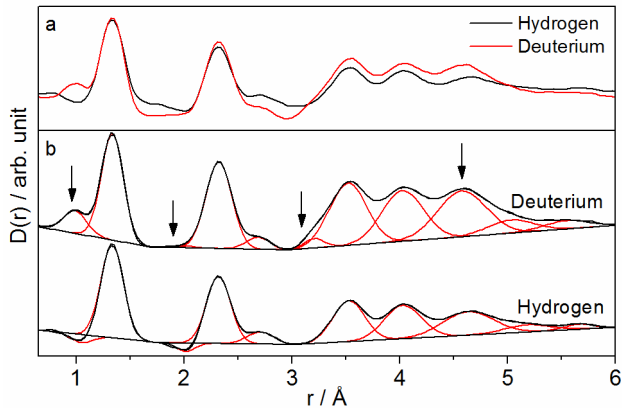


Figure 8  $D(r)$  of graphitic carbon nitride and of the deuterated analogue.

Figure 9 compares the experimental correlation function to the theoretical  $D(r)$  of the structures selected after the x-ray diffraction investigation: the modified Melon, the structures with  $\alpha$  and  $\beta \neq 90^\circ$  and the structure with shifted layers (Shift A). After generating the theoretical  $D(r)$  plots the area ratios  $A_{\text{peak}}/A_{1.33}$  are used to compare the different structures, together with the  $R_w$  values. The modelling of an amorphous material is less accurate at large distances (section III in Figure 7). For this reason here the  $R_w$  values are given for the shorter range, 0-6 Å.

The theoretical  $D(r)$  of the modified version of Melon well matches the measured one up to 3 Å (Figure 9a). Above this value it cannot be considered satisfactory. Table 1 shows the relative peak areas of the theoretical pattern. The ratio  $A_{2.1}/A_{1.33} = 1.23$  is comparable to that of the measured  $D(r)$  (1.25). However, the relative peak area of the correlation at 1.03 Å is higher than the measured value suggesting a higher content of N-H bonds in the modelled structure compared to the real structure. Another difference is found at 4.62 Å. This feature is found significantly lower ( $A_{4.62}/A_{1.33} = 0.39$ ) than the experimental value of 0.77. In addition, the correlation at 5.14 Å appears almost missing with an  $A_{5.14}/A_{1.33} = 0.05$ . The  $R_w$  for this model is found to be 0.41.

Among the models with modified  $\alpha$  and  $\beta$ , the angles  $92^\circ$ ,  $95^\circ$  and  $98^\circ$  were employed to generate the theoretical  $D(r)$ . Among them the models with  $\alpha$  or  $\beta$  of  $98^\circ$  produced the best result (Table 1 and Table S4). The theoretical  $D(r)$  of the two models are illustrated in Figure 9b and Figure 9c. The results for both structures are very similar. In both cases an  $R_w$  of 0.40 is obtained. The correlation at 1.03 Å is still characterised by a relative area which is too high. Even though an angle different from  $90^\circ$  brings to a small increase in the ratio  $A_{\text{VII}}/A_{\text{II}}$ , now equal to 0.54 for  $\alpha$  and 0.64 for  $\beta$ , this remains too small if compared to the experimental value. Similarly, the correlation at 5.14 Å is still found with a low relative peak area (0.06 for  $\alpha$  and 0.02 for  $\beta$ ).

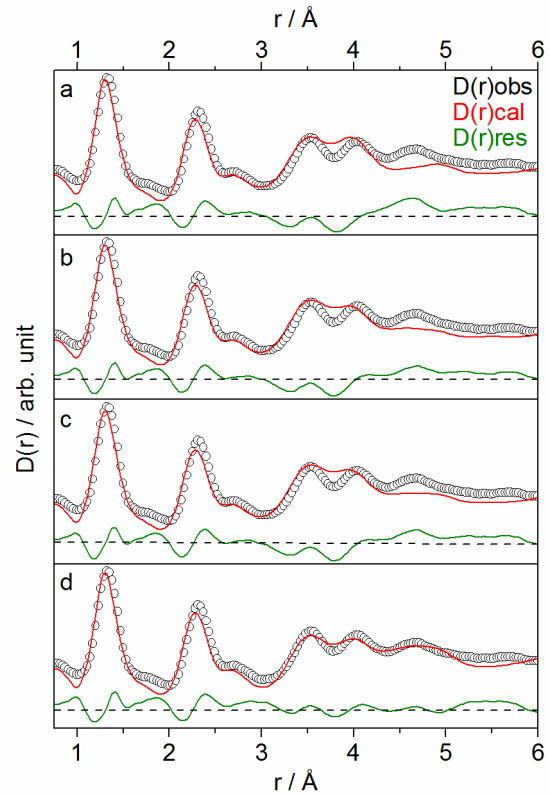


Figure 9 Comparison between the calculated  $D(r)$  and the observed  $D(r)$ . The residual represents the difference between the two curves. a) Modified Melon, b)  $\alpha = 98^\circ$ , c)  $\beta = 98^\circ$  and d) Shift A.

When an actual shift of the layers (Shift A) is introduced in the structure, the  $R_w$  decreases to a value of 0.32 (Table 1). The calculated  $D(r)$  for the structure is presented in Figure 9d. It readily be seen that the calculated  $D(r)$  well matches the observed  $D(r)$ . Even though an excess of N-H bonds is still present ( $A_{\text{I}}/A_{\text{II}} = 0.15$ ) all the other correlations have relative areas that match those of the measured  $D(r)$ . In particular in the region of the *inter-layer* interactions, the correlations at 4.62 Å and 5.14 Å are now characterized by values which are very close to the experimental ones.

To account for a higher level of polymerisation than that of Melon a mixed phase is also considered. The modelled structure with shifted layers is taken as main phase and a fully polymerised tri-*s*-triazine structure with A-B stacking is added to the model. In order to find the composition of the mixture, this was refined until constant  $R_w$ . The lowest achievable  $R_w$  of 0.27 was obtained for a mixture of 70 % of shifted Melon and 30 % of the fully polymerised structure.

**Table 1 Summary of the Normalized Peak Areas As Obtained from the Gaussian Fitting of the D(r) From g-C<sub>3</sub>N<sub>4</sub>H<sub>x</sub> Prepared From Melamine Fired at 500 °C for 15 h**

r (Å)	A <sub>peak</sub> /A <sub>1,33</sub>				
	g-C <sub>3</sub> N <sub>4</sub>	Melon	α = 98 °	β = 98 °	Shift A
1.03	0.07	0.15	0.14	0.15	0.15
2.07	0.14	0.09	0.09	0.09	0.08
2.1	1.25	1.23	1.24	1.23	1.29
2.72	0.14	0.12	0.12	0.12	0.15
3.52	0.63	0.64	0.69	0.65	0.67
4.03	0.59	0.72	0.60	0.64	0.61
4.62	0.77	0.39	0.54	0.64	0.8
5.14	0.20	0.05	0.06	0.02	0.23
R <sub>w</sub>	-	0.41	0.40	0.40	0.32

## DISCUSSION

After an initial investigation by XRD followed by a neutron diffraction study, the following observations can be made. The structure of g-C<sub>3</sub>N<sub>4</sub> calculated by Teter and Hemely and officially recognised does not describe the photoactive material (g-C<sub>3</sub>N<sub>4</sub>) obtained by calcination of small organic molecules, in the specific melamine. The *inter*-layer *d*-spacing of Teter and Hemley's structure is too large (0.336 nm) compared to that of the synthesised material (0.326 nm). Furthermore, the theoretical pattern does not justify the peak observed at ~13°. A tri-*s*-triazine-based structure produces a XRD pattern similar to the measured one suggesting that indeed the structure is based on the tri-*s*-triazine building block.

The removal of some of the tri-*s*-triazine units from the polymeric network, in order to introduce hydrogen atoms, does not bring an improved result. Too many reflections at low angles are present, making these partially polymerised structures not representative of the here synthesised material. However, the structure proposed by Lotsch *et al.*<sup>16, 20</sup>, Melon, produces a theoretical XRD pattern that well matches the experimental one in terms of peak position with only a small shift of the (210)<sub>orthorhombic</sub> reflection. The structure consists of parallel chains of tri-*s*-triazine units and can be classified as partially polymerised. The elemental composition (C<sub>2.88</sub>N<sub>4.32</sub>H<sub>1.44</sub>) of Melon and the C:N ratio (0.67) are coherent with those measured for the material synthesised for this study (C<sub>2.88</sub>N<sub>4.23</sub>H<sub>1.51</sub> and 0.68).

Due to the close match of the XRD pattern and the similar atomic composition, this structure is employed here as a starting point for further modifications. This can be justified by the different synthetic method employed by Lotsch *et al.*<sup>16, 20</sup> which generates a more ordered structure. To bring the position of the (210) reflection to the desired value the unit cell parameter *a* is decreased by

moving the chains closer to each other. The position of the (210) reflection of the modified-Melon matches the position of the experimental one. However, the relative intensity is too high compared to the measured peak. The intensity of this reflection is most likely linked to 3D structural features that can be affected by the synthesis method. In fact, Tyborsky *et al.* after a double calcination step obtained a peak at ~13° that is more intense and defined than that of the g-C<sub>3</sub>N<sub>4</sub> synthesised for this study. An example of structural effect is a shift of the aromatic layers. A misalignment of the layers can affect the intensity of the (210) reflection. A shift of the layers is simulated by changing the angle α or β in the unit cell, which will become monoclinic. A change in one of these angles shows that it is possible to decrease the intensity of the (210) reflection but also move the reflection towards higher angles. The optimum range for both angles is found to be between 82° and 98°.

To introduce a shift of the layers the vectors proposed by Lostch are applied on the atomic coordinates of the modified Melon. Indeed shifting the layers produces a decrease in the intensity of the (210) reflection. The most effective shift is Shift A, offset stacking of the layers, thermodynamically favourable. The aromatic layers are surrounded by π clouds. If the layers are perfectly aligned this will create repulsive forces. However, an off-set between the layers minimizes the π-π *inter*-layer interactions, making the structure more stable and therefore more likely to be formed during the thermal polycondensation process. Shift A is the most successful model because it brings the tri-*s*-triazine units of a layer to be in between two tri-*s*-triazine units of an adjacent layer, creating an optimum A-B configuration that minimises the repulsion of the layers (Figure S3a). These results are confirmed by the neutron diffraction analysis that shows that among the considered models, Shift A produces a calculated D(r) that best matches the measured one.

To account for the lower amount of N-H bonds found in the measured D(r) compared to the calculated ones, a mixture of shifted Melon and a fully polymerised tri-*s*-triazine structure was considered. A marginally better R<sub>w</sub> is obtained when 30% of the fully polymerised structure is added as a secondary phase. This high amount is however surprising since the atomic composition for the modelled Melon (C<sub>2.88</sub>N<sub>4.32</sub>H<sub>1.44</sub>) is found coherent with the values measured for the synthesised material (C<sub>2.88</sub>N<sub>4.23</sub>H<sub>1.51</sub>). Therefore, it can be assumed that the peak at 1.03 Å is artificially affected by the correction for inelastic scattering characteristic of hydrogen atoms.

## CONCLUSIONS

In conclusion the structure of a photocatalytically active graphitic carbon nitride synthesised via polycondensation of melamine was investigated by mean of XRD and neutron diffraction. In both cases modelled structures were employed to generate calculated patterns and plots. These were then compared to the measured ones. Starting

from proposed structural models for graphitic carbon nitride, we reduced to one the number of 3D configurations that can describe the structure of our catalyst. From the results it can be concluded that graphitic carbon nitride obtained from calcination of melamine in a closed system is a tri-s-triazine based polymer organised in layers at a distance of 0.326 nm. These layers, however are not aligned with an A-A configuration but they present an off-set with respect to each other. This A-B configuration sees tri-s-triazine of adjacent layers being alternated. This minimises the repulsive forces of the  $\pi$  clouds of adjacent layers. We believe that this work, by using neutron diffraction for the first time on graphitic carbon nitride, provides important insights on the 3D structure of photoactive g-C<sub>3</sub>N<sub>4</sub> synthesised via thermal polycondensation of melamine.

## ASSOCIATED CONTENT

**Supporting Information.** Atomic coordinates, graphical information additional neutron diffraction summary. This material is available free of charge via the Internet at <http://pubs.acs.org>.

## AUTHOR INFORMATION

### Corresponding Author

\* Tel: +44 (0)1334 463817. E-mail: [jtsi@st-andrews.ac.uk](mailto:jtsi@st-andrews.ac.uk)

### Author Contributions

F.F. wrote the manuscript and carried out the XRD and neutron diffraction modelling. S.K.C. was the instrument scientist for the neutron scattering experiment. G.M.C. helped in the preparation of the samples and in the acquisition of the data. F.F. and J.T.S.I. designed the experiments. All authors have given approval to the final version of the manuscript.

## ACKNOWLEDGMENT

We thank EPSRC for support through the EPSRC/NSF chemistry programme and the Royal Society for a Wolfson Merit award.

## REFERENCES

- Liebig, J., *Annalen der Pharmacie* **1834**, 10 (1), 1-47.
- Wang, X.; Maeda, K.; Thomas, A.; Takanabe, K.; Xin, G.; Carlsson, J. M.; Domen, K.; Antonietti, M., *Nat. Mater.* **2009**, 8 (1), 76-80.
- Thomas, A.; Fischer, A.; Goettmann, F.; Antonietti, M.; Müller, J.-O.; Schlogl, R.; Carlsson, J. M., *J. Mater. Chem.* **2008**, 18 (41), 4893-4908.
- Wang, Y.; Wang, X.; Antonietti, M., *Angewandte Chemie International Edition* **2012**, 51 (1), 68-89.
- Franklin, E. C., *J. Am. Chem. Soc.* **1922**, 44 (3), 486-509.
- Pauling, L.; Sturdivant, J. H., *Proc. Natl. Acad. Sci. U. S. A.* **1937**, 23 (12), 615-620.
- Redemann, C. E.; Lucas, H. J., *J. Am. Chem. Soc.* **1940**, 62 (4), 842-846.
- Teter, D. M.; Hemley, R. J., *Science* **1996**, 271, 53-55.
- Matsumoto, S.; Xie, E. Q.; Izumi, F., *Diamond Relat. Mater.* **1999**, 8 (7), 1175-1182.
- Kawaguchi, M.; Nozaki, K., *Chem. Mater.* **1995**, 7 (2), 257-264.
- Gillan, E. G., *Chem. Mater.* **2000**, 12 (12), 3906-3912.
- Kroke, E.; Schwarz, M., *Coord. Chem. Rev.* **2004**, 248 (5-6), 493-532.
- Jürgens, B.; Irran, E.; Senker, J.; Kroll, P.; Müller, H.; Schnick, W., *J. Am. Chem. Soc.* **2003**, 125 (34), 10288-10300.
- Yan, S. C.; Li, Z. S.; Zou, Z. G., *Langmuir* **2009**, 25 (17), 10397-10401.
- Groenewolt, M.; Antonietti, M., *Adv. Mater.* **2005**, 17 (14), 1789-1792.
- Lotsch, B. V.; Döblinger, M.; Sehnert, J.; Seyfarth, L.; Senker, J.; Oeckler, O.; Schnick, W., *Chem. - Eur. J.* **2007**, 13 (17), 4969-4980.
- Lotsch, B. V.; Schnick, W., *Chem. Mater.* **2006**, 18 (7), 1891-1900.
- Lotsch, B. V.; Schnick, W., *Chem. Mater.* **2005**, 17 (15), 3976-3982.
- Döblinger, M.; Lotsch, B. V.; Wack, J.; Thun, J.; Senker, J.; Schnick, W., *Chem. Commun.* **2009**, (12), 1541-1543.
- Lotsch, B. V. PhD Thesis, Ludwig-Maximilian University of Munich, 2006.
- Tyborski, T.; Merschjann, C.; Orthmann, S.; Yang, F.; Lux-Steiner, M.-C.; Schedel-Niedrig, T., *J. Phys.: Condens. Matter* **2013**, 25 (39), 395402.
- Keen, D., *J. Appl. Cryst.* **2001**, 34 (2), 172-177.
- Sears, V. F., *Neutron News* **1992**, 3 (3), 26-37.
- Soper, A. K.; Science; Council, T. F., *GudrunX and GudrunX: Programs for Correcting Raw Neutron and X-ray Diffraction Data to Differential Scattering Cross Section*. Science & Technology Facilities Council: 2011.
- Farrow, C. L.; Juhas, P.; Liu, J. W.; Bryndin, D.; Božin, E. S.; Bloch, J.; Proffen, T.; Billinge, S. J. L., *J. Phys.: Condens. Matter* **2007**, 19 (33), 335219.
- Lide, D. R., *CRC Handbook of Chemistry and Physics*. 71st ed.; CRC Press, Boca Raton: 1990.
- Kroke, E.; Schwarz, M.; Horath-Bordon, E.; Kroll, P.; Noll, B.; Norman, A. D., *New J. Chem.* **2002**, 26 (5), 508-512.
- Allen, F. H.; Kennard, O.; Watson, D. G.; Brammer, L.; Orpen, A. G.; Taylor, R., *J. Chem. Soc., Perkin Trans. 2* **1987**, (12), S1-S19.



---

Graphic entry for the Table of Contents (TOC)

